



OPEN

# FGF23 neutralization improves bone quality and osseointegration of titanium implants in chronic kidney disease mice

SUBJECT AREAS:

KIDNEY

BONE

EXPERIMENTAL MODELS OF  
DISEASENingyuan Sun<sup>1</sup>, Yuchen Guo<sup>1</sup>, Weiqing Liu<sup>1</sup>, Michael Densmore<sup>2</sup>, Victoria Shalhoub<sup>3\*</sup>,  
Reinhold G. Erben<sup>4</sup>, Ling Ye<sup>1</sup>, Beate Lanske<sup>2</sup> & Quan Yuan<sup>1,2</sup>Received  
28 August 2014Accepted  
16 December 2014Published  
10 February 2015Correspondence and  
requests for materials  
should be addressed to  
Q.Y. (yuanquan@scu.  
edu.cn)\* Current address:  
Siemens Healthcare  
Diagnostics Inc.,  
Tarrytown, NY

<sup>1</sup>State Key Laboratory of Oral Diseases, West China Hospital of Stomatology, Sichuan University, Chengdu, China, <sup>2</sup>Department of Oral Medicine, Infection, and Immunity, Harvard School of Dental Medicine, Boston, MA, <sup>3</sup>Amgen Inc., Thousand Oaks, CA, USA, <sup>4</sup>Department of Biomedical Sciences, University of Veterinary Medicine, Vienna, Austria.

Chronic kidney disease (CKD) is a worldwide health problem. Serum levels of FGF23, a phosphaturic hormone, increase at the earliest stages of CKD, and have been found to be independently associated with the mortality and morbidity of CKD patients. The purpose of this study was to evaluate whether FGF23 neutralization was able to improve bone quality and osseointegration of titanium implants. Uremia was induced by 5/6 nephrectomy in adult female mice. Postsurgery, the mice were injected with vehicle or FGF23 neutralizing antibody (5 mg/kg body weight) 3 times a week. Experimental titanium implants were inserted in the distal end of the femurs. FGF23 neutralization significantly increased serum phosphate, 1,25(OH)<sub>2</sub>D and BUN, and decreased serum PTH and FGF23, relative to vehicle-treated CKD mice. Histomorphometric analysis of the tibiae indicated that FGF23 neutralization normalized the osteoidosis observed in vehicle-treated CKD mice. Although bone-implant contact ratio remained unchanged by anti-FGF23 antibody treatment, the strength of osseointegration, as evidenced by a biomechanical push-in test, was significantly improved by FGF23 neutralization. Our findings revealed that FGF23 neutralization effectively improves bone quality and osseointegration of titanium implants in CKD mice, suggesting FGF23 as a key factor of CKD related bone diseases.

Chronic kidney disease (CKD) has become a worldwide health problem with rapidly growing prevalence<sup>1</sup>. A previous cross-sectional survey in Chinese and Bangladesh adults showed that the overall prevalence of CKD was 10.8% and 26%, respectively<sup>2,3</sup>. A similar situation is found in developed countries: The prevalence of CKD in USA and Norway was reported as 13.0% and 10.2%, respectively<sup>4,5</sup>.

Declining renal function impairs the normal physiological mechanisms regulating blood levels of calcium, phosphate, fibroblast growth factor 23 (FGF23), parathyroid hormone (PTH), and vitamin D. These hormonal imbalances negatively impact on bone structural integrity, and subsequently lead to chronic kidney disease-mineral and bone disorders (CKD-MBD). KDIGO's clinical guidelines pointed out that 84% of CKD patients reveal histological evidence of bone disease<sup>6</sup>. Patients with predialysis CKD and fractures show lower bone mineral density (BMD), thinner cortices, and trabecular loss<sup>7</sup>. Lobão *et al.* reported that nearly half of the predialysis CKD participants with median creatinine clearance of 29 ml/min/1.73 m<sup>2</sup> display low bone mineral density<sup>8</sup>. Our previous study also demonstrated that chronic kidney disease impaired bone-implant contact (BIC) ratio and strength of bone-implant integration in CKD mice<sup>9</sup>.

Fibroblast growth factor 23 (FGF23), a phosphaturic hormone secreted mostly by mature osteoblasts and osteocytes, plays a major role in regulating mineral ion homeostasis<sup>10–12</sup>. The alteration of FGF23 expression causes disturbances in phosphate metabolism, which may subsequently lead to hyperphosphatemia or rickets<sup>10,13,14</sup>. Apart from that, FGF23 plays a direct role of inhibiting mineralization as demonstrated by a study using adenoviral overexpression of FGF23 in rat calvarial cells<sup>15</sup>. Shalhoub and colleagues also demonstrated that the presence of FGF23 and its coreceptor, Klotho, resulted in inhibition of mineralization and osteoblast activity<sup>16</sup>.

It is well-known that serum fibroblast growth factor 23 (FGF23) is already elevated at the early stages of CKD<sup>17,18</sup>, and that circulating FGF23 levels are correlated with renal creatinine clearance<sup>17</sup>. FGF23 was shown to be independently associated with mortality and morbidity in CKD patients, including therapy-resistant secondary hyperparathyroidism, impaired vasoreactivity, arterial stiffness and calcitriol deficiency<sup>19–21</sup>. In addition,



FGF23 is independently associated with chronic kidney disease-mineral and bone disorder (CKD-MBD) in CKD patients<sup>22,23</sup>.

A recent study has shown that FGF23 neutralization is, to some extent, able to ameliorate the levels of parathyroid hormone, vitamin D, serum calcium, and to normalize bone markers in uremic rats<sup>24</sup>. We hypothesized that the elevated FGF23 levels in CKD patients impair bone structure and quality, which in turn can be an obstacle to the osseointegration of titanium dental implants. To test this hypothesis, we used FGF23 antibody to neutralize the function of FGF23, and investigated trabecular bone turnover and osseointegration of a titanium implant in a CKD mouse model.

## Methods

**Ethics Statement.** This study was performed in strict accordance with the recommendations contained in the Guide for the Care and Use of Laboratory Animals of the National Institutes of Health and the ARRIVE guidelines (<http://www.nc3rs.org.uk/arrive-guidelines>). All of the experiments carried out were approved by the Subcommittee on Research and Animal Care (SRAC), which serves as the Institutional Animal Care and Use Committee (IACUC) at the Harvard Medical School (protocol number: 03901). All surgery was performed under anesthesia by intraperitoneal injection of a combination of ketamine (100 mg/ml) and xylazine (10 mg/ml), in addition, buprenorphine (0.05 mg/kg) was given for perioperative analgesia to minimize suffering and pain.

**Animals.** Nine-week-old female C57BL mice were purchased from Charles River Laboratories International Inc. (Wilmington, MA). The animals were kept under climate-controlled conditions and fed with standard diet. All studies were approved by the Institutional Animal Care and Use Committee at the Harvard Medical School (Boston, MA). The mice were randomly divided into 4 groups, and each group contained 8 animals.

**Surgical procedure to induce uremia.** The CKD mice were established by a two-step 5/6 nephrectomy to induce uremia as described previously<sup>9</sup>. Briefly, the left kidney was approached through a 2-cm-long lumbar incision and exposed by fine dissection of the peri-renal fat and adrenal gland. The left kidney was cauterized except for a 2-mm area around the hilum. The kidney was then returned to the renal fossa, and the subcutaneous tissues were sutured with 6-0 silk. The skin was closed with surgical clips. After 1 week, a total nephrectomy of the right kidney was performed by ligation of the renal hilum with a 5-0 silk suture and surgical excision of the kidney. The wound was closed as the first surgery. Sham surgery consisted of anesthetic, flank incision exposing the kidney, and closure of the abdominal wall.

**Administration of neutralizing FGF23 antibody.** Neutralizing FGF23 Ab was kindly provided by Amgen Inc. (Thousand Oaks, CA)<sup>24</sup>. It was diluted in PBS and administered intraperitoneally 3 times per week (5 mg/kg body weight). The administration was started 8 weeks after the second renal surgery and continued for a period of 4 weeks. An illustration of the workflow is shown in Figure 1. Day 0 of the study is defined as the date of the second renal ablation.

**Implant surgery.** Ten weeks after the second renal ablation surgery, the mice were subjected to implant placement by the method described previously<sup>9</sup>. Titanium implants with SLA surface (1 mm in diameter and 4 mm in length) were kindly provided by Institut Straumann AG (Basel, Switzerland). They were cut to the length of 2 mm before insertion. The distal aspect of the femurs was carefully exposed after the skin incision and fine muscle dissection. The implant site was prepared on the medial surfaces of each femur by sequential drilling with 0.7- and 1.0-mm surgical stainless steel twist drills. The implant was press-fitted into the hole for primary stability. After the insertion of the implant, the muscles were carefully sutured with 6-0 silk, which covered the implant and further guaranteed its protection in the biological environment. Then the skin was closed with 5-0 silk. Eight mice were allocated to each group.

**Serum biochemical assays.** Twelve weeks after the second renal surgery, blood was collected by cheek pouch before sacrifice of the mice. Serum biochemistry was performed using commercially available kits: Blood urea nitrogen (BUN) (Stanbio Laboratory, Boerne, TX); FGF23 (Immutopics, San Clemente, CA, Cat.#60-6300),

PTH (Immutopics, San Clemente, CA); 1,25(OH)<sub>2</sub>D (Immunodiagnostic Systems Ltd., Fountain Hills, AZ); Calcium and Phosphate (Stanbio Laboratory, Boerne, TX).

**Histological preparation and histomorphometric measurement.** The processing of undecalcified bone specimens and cancellous bone were performed as described previously<sup>9,25</sup>. Femurs and tibiae were fixed in 10% buffered formalin at 4°C overnight and stored in 70% ethanol at 4°C. Specimens were exposed to X-ray (20 kV, 5 seconds) before being processed.

The total mineral content (TOT\_CNT) and mineral density (TOT\_DEN) of proximal tibiae were assessed by peripheral quantitative computerized tomography (pQCT), as described previously<sup>26</sup>. Then the tibiae were embedded in methylmethacrylate and three- $\mu$ m-thick midsagittal sections were prepared using a HM 360 microtome (Microm, Walldorf, Germany). Histomorphometric measurements in the proximal ends were made on sections stained with von Kossa/McNeal using a semiautomatic system (OsteoMeasure, OsteoMetrics, Decatur, GA), and a Zeiss Axioskop microscope with a drawing attachment. The area within 0.25 mm of the growth plate was excluded from the measurements. All histomorphometric parameters were calculated and expressed according to the suggestions made by the ASBMR nomenclature committee<sup>27</sup>.

The left side of the femur carrying an implant from each mouse was dehydrated and embedded in light-curing epoxy resin (Technovit 7200VLC, HereausKulzer, Wehrheim, Germany). Embedded specimens were sawed perpendicular to the longitudinal axis of the implants at a site 0.5 mm from its apical end. Then the specimens were ground to about 50  $\mu$ m thickness with a grinding system (Exakt Apparatebau, Norderstedt, Germany). Sections were stained with Stevenel's blue and Van Gieson's picro-fuchsin, and histomorphometrically analyzed with NIH Image J (National Institutes of Health, USA). BIC was calculated as the linear percentage of direct bone-to-implant contact to the total surface of the implant.

**Implant biomechanical push-in test.** The right side of the femur containing a cylindrical implant from each mouse was harvested and embedded into autopolymerizing resin with the top surface at the implant level. A testing machine (AG-TA electronic universal testing machine, SHIMADZU, Japan) equipped with a pushing rod (diameter = 0.8 mm) was used to load the implant vertically downward at a crosshead speed of 1 mm/min. The push-in value was determined by measuring the peak of the load-displacement curve.

**Statistical analysis.** All values are presented as mean  $\pm$  SD. Statistically significant differences were assessed by ANOVA followed by Turkey's multiple comparisons, or by independent student *t* test for comparisons between two groups. A *p* value of less than 0.05 was considered to be statistically significant.

## Results

**Serum biochemistry.** Significant differences were observed between the sham + vehicle group and the CKD + vehicle group in terms of serum BUN (Fig. 2A), FGF23 (Fig. 2D), PTH (Fig. 2E), and Vit D (Fig. 2F), indicating successful establishment of the uremic mouse model. Injection of FGF23 Ab did not change the BUN levels in the normal mice, but further elevated the levels in CKD mice from 43.87  $\pm$  5.33 mg/dl to 65.62  $\pm$  11.17 mg/dl ( $p < 0.05$ ). The serum calcium levels remained stable (Fig. 2B), while the phosphate levels were significantly increased in both sham and CKD mice after FGF23 Ab injection (Fig. 2C). The serum FGF23 level in the CKD mice was over 2-fold higher than that of control, and it was restored to the normal level after FGF23 Ab administration (Fig. 2D). Similarly, the hyperparathyroidism observed in the CKD mice was significantly decreased after FGF23 Ab treatment (Fig. 2E). As shown in Fig. 2F, serum 1,25(OH)<sub>2</sub>D in CKD mice was significantly lower than that of sham group. FGF23 Ab injection significantly elevated serum 1,25(OH)<sub>2</sub>D both in the sham and CKD mice.

**FGF23 neutralizing improved bone quality.** We then analyzed the response to FGF23 treatment in bone by comparing the proximal tibiae using ex vivo pQCT. No significant difference was observed in

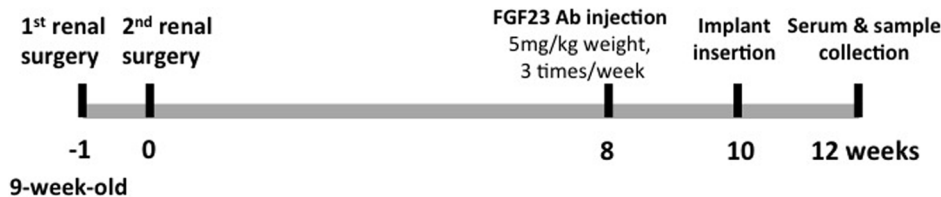


**Figure 1** | Illustration of the workflow.

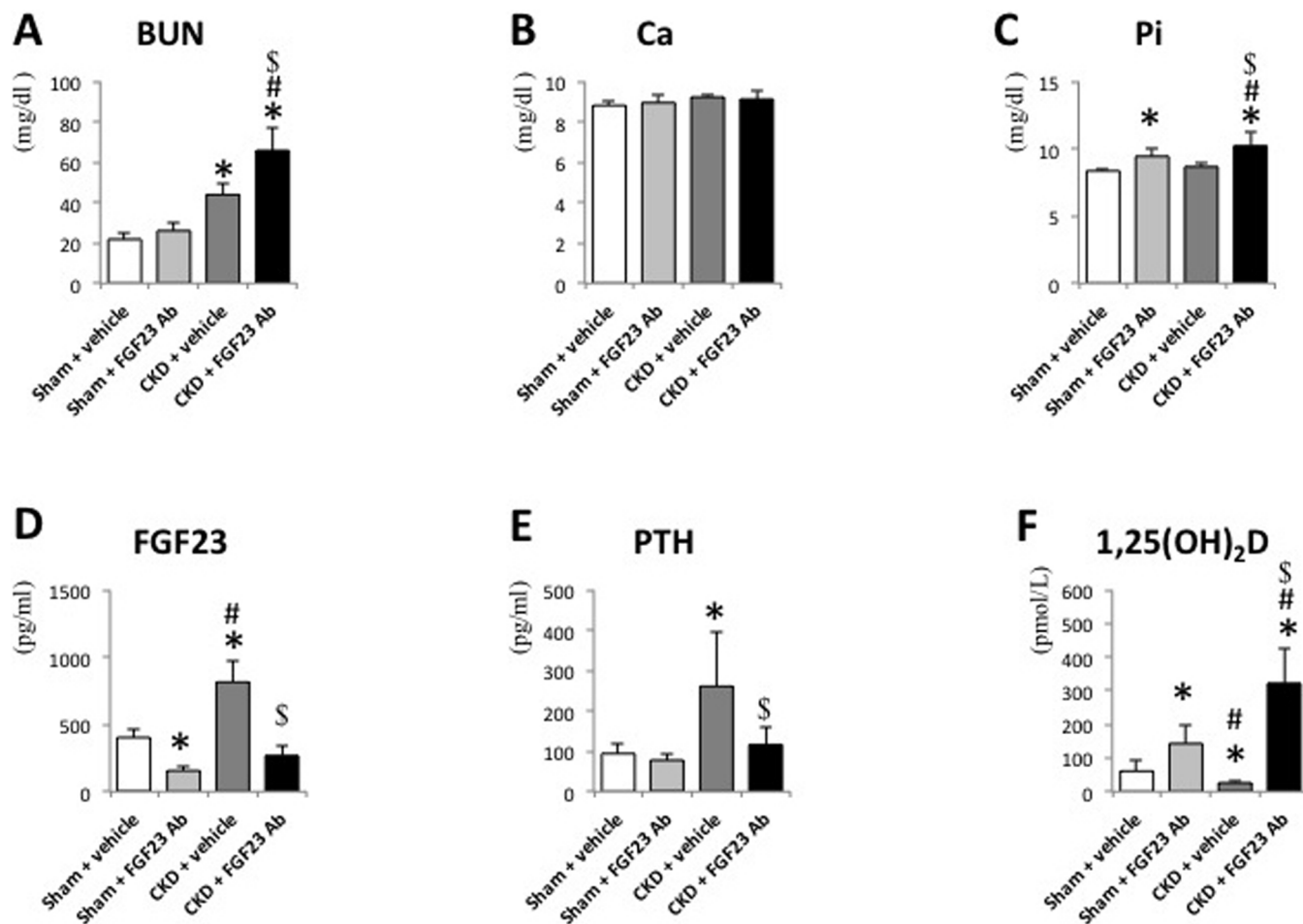


**Figure 2 | Serum biochemical measurements.** (A) serum BUN; (B) serum calcium; (C) Serum phosphate; (D) serum FGF23; (E) serum PTH and (F) serum 1,25(OH)<sub>2</sub>D. \*:  $p < 0.05$  vs Sham + vehicle; #:  $p < 0.05$  vs Sham + FGF23 Ab; \$:  $p < 0.05$  vs CKD + vehicle.

terms of total mineral content (TOT\_CNT) and total mineral density (TOT\_DEN) between the sham and CKD mice (Fig. 3A&B). FGF23 Ab injection seemed to induce a slight increase of TOT-DEN (Fig. 3B), however there were no significant differences among the four groups in both TOT-CNT and TOT-DEN.

Fig. 4A shows the histological images of undecalcified sections stained with von Kossa and McNeal blue. Increased trabecular bone volume (BV/TV) was observed in CKD mice, but it was restored to a level comparable to that of normal mice after FGF23 Ab administration (Fig. 4B). FGF23 Ab injection also

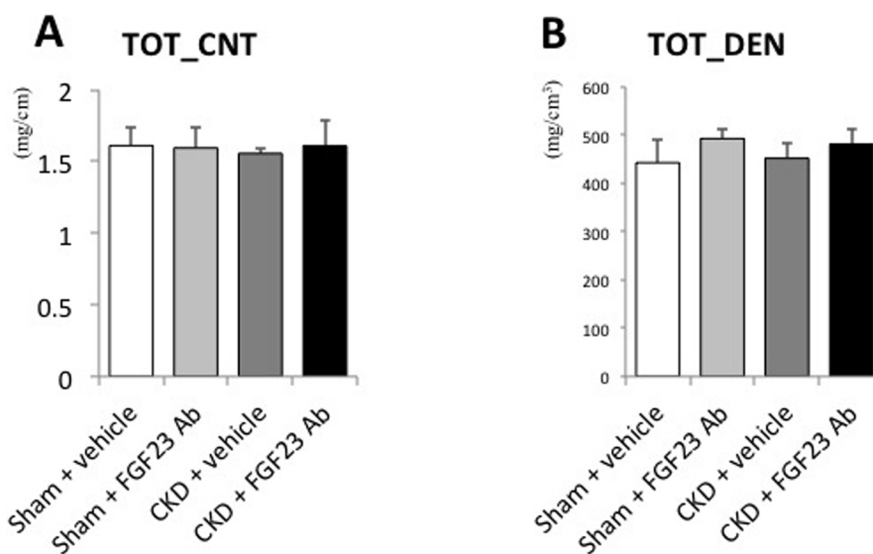


**Figure 3 | Measurement of bone density of proximal tibiae.** (A) total mineral content (TOT\_CNT); and (B) total mineral density (TOT\_DEN).

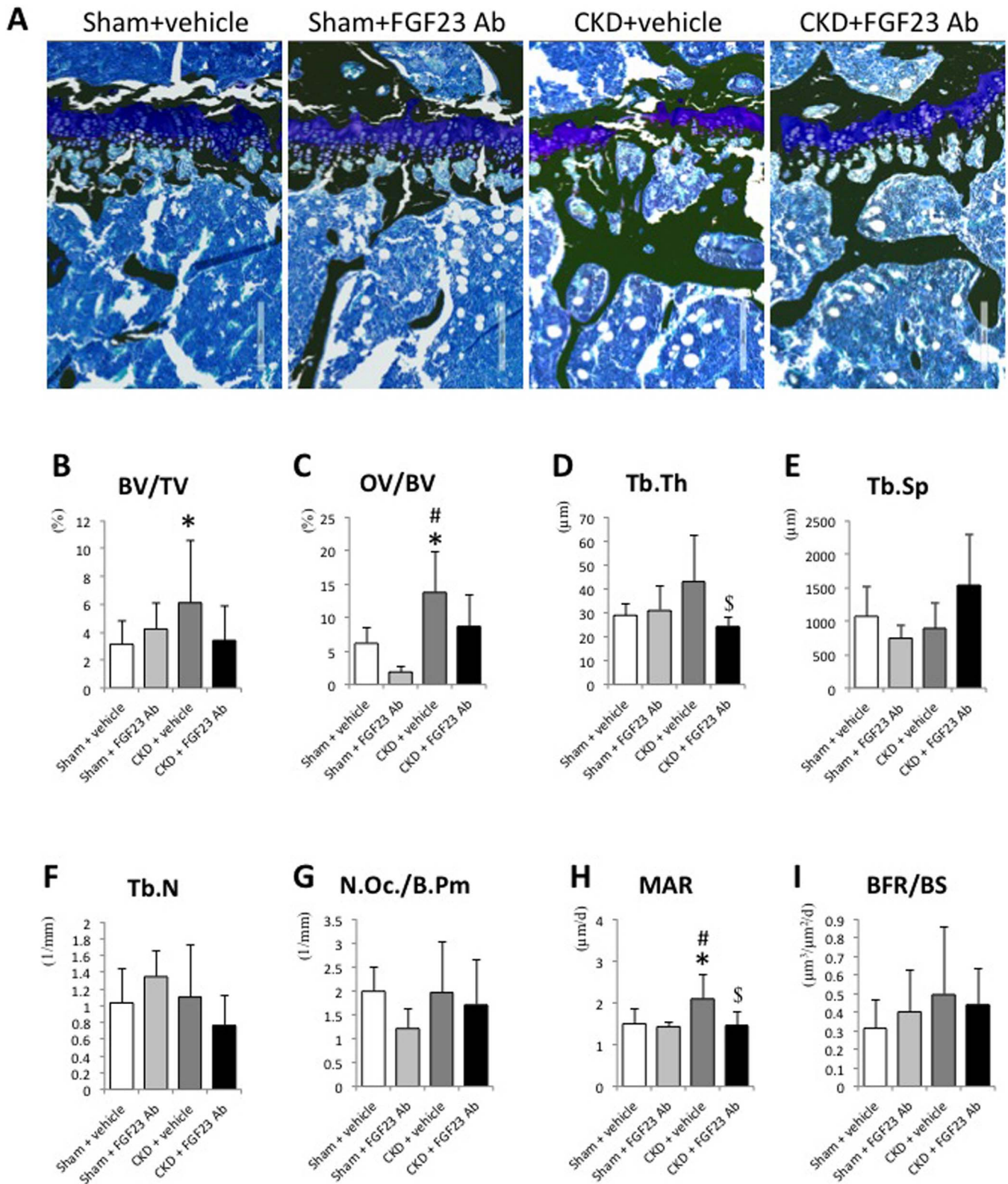


**Figure 4 | Histological and histomorphometric analyses.** (A) Representative images of undecalcified sections of the proximal ends of tibiae stained with von Kossa and McNeal stains; (B) BV/TV=bone volume; (C) OV/TV=osteoid volume; (D) Tb.Th=trabecular thickness; (E) Tb.Sp=trabecular separation; (F) Tb.N=trabecular number; (G) N.Oc./B.Pm=osteoclast number/bone perimeter (H) MAR=mineral apposition rate; (I) BFR=bone formation rate. \*:  $p < 0.05$  vs Sham + vehicle; #:  $p < 0.05$  vs Sham + FGF23 Ab; \$:  $p < 0.05$  vs CKD + vehicle.

improved the osteoid volume (OV/TV) and trabecular thickness (Tb.Th). There are no significant differences in the trabecular separation (Tb.Sp), trabecular number (Tb.N) and number of

osteoclasts per bone perimeter (N.Oc./B.Pm) among all four groups (Fig. 4E–G). Moreover, we observed that FGF23 neutralization corrected the increased mineral apposition rate (MAR) in

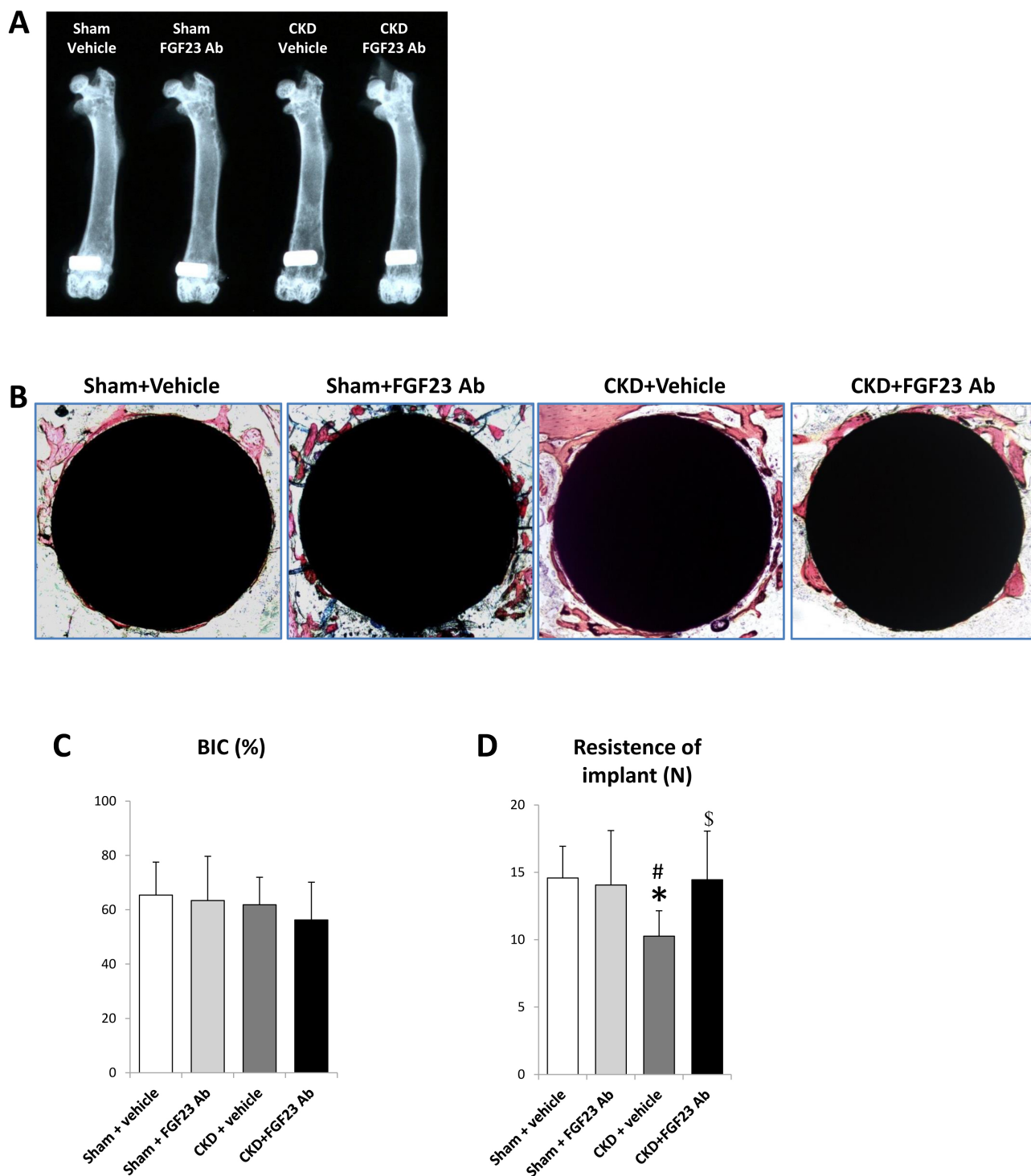


**Figure 5 | Histological and biomechanical analysis.** (A) X-ray examination of the femurs with implants. (B) Undecalcified sections stained with Stevenel's blue and Van Gieson's picro-fuchsin; (C) Bone-implant contact ratio (BIC, %); (D) push-in resistance of the implants. \*:  $p < 0.05$  vs Sham + vehicle; #:  $p < 0.05$  vs Sham + FGF23 Ab; \$:  $p < 0.05$  vs CKD + vehicle.

CKD mice (Fig. 4H), while no significant difference was found for bone formation rate (BFR) (Fig. 4I).

**FGF23 neutralizing increased fixation of titanium implants.** As anticipated, all mice survived the observation period and no inflammation at the implant site was observed. The *ex vivo* X-ray examination of the femurs showed that the implants were surrounded with bone without any notable gap, indicating successful osteointegration for both groups (Fig. 5A).

The observation of histological sections confirmed a direct bone-implant contact for all four groups (Fig. 5B). Further histomorphometrical analyses did not reveal any statistically significant differences for peri-implant BIC ratio (Fig. 5C). Consistent with our previous report, CKD mouse showed significantly impaired push-in resistance of the titanium implants ( $p < 0.05$ ) (Fig. 5D). However, it was significantly increased after FGF23 Ab treatment ( $14.45 \pm 3.61$  N) ( $p < 0.05$ ), compared to that of vehicle ( $10.26 \pm 1.89$  N), indicating an improvement of bone-implant integration (Fig. 5D).



## Discussion

In the study, we established a CKD mouse model that was subsequently treated with FGF23 antibody to investigate the effect of FGF23 neutralization on serum changes, bone structure and implant fixation. The treatment successfully neutralized the elevated FGF23 levels, corrected the secondary hyperparathyroidism, and elevated 1,25(OH)<sub>2</sub>D levels as well. More importantly, the neutralization of FGF23 clearly normalized the bone structure of CKD mice, including the BV/TV, OV/TV, Tb.Th and MAR. FGF23 Ab administration also improved the push-in resistance of the implants. These results indicate that FGF23 plays a key role in CKD related bone diseases.

Vit D is a fundamental micronutrient with major implications for human health<sup>28</sup>. Vit D deficiency, which is defined as a 25(OH)<sub>2</sub>D level of less than 20 ng/ml (50 nmol per liter), is highly prevalent in patients with CKD<sup>29</sup>. Aberrant Vit D metabolism in CKD including decreased synthesis in the skin and urinary loss of Vit D metabolites contribute to this high prevalence<sup>30,31</sup>. Since the reduction in renal function also diminishes the activity of 1 $\alpha$ -hydroxylase (1 $\alpha$ -OHase), the enzyme that converts 25(OH)<sub>2</sub>D to its activated form, 1,25(OH)<sub>2</sub>D. Serum level of 1,25(OH)<sub>2</sub>D of CKD + vehicle group decreased significantly compared with sham + vehicle group, however, this parameter increased significantly after FGF23 Ab administration. A major biological function of 1,25(OH)<sub>2</sub>D is to maintain proper serum phosphorus and calcium concentrations in order to support cellular functions and to promote mineralization of the skeleton<sup>32</sup>. Vitamin D deficiency causes secondary hyperparathyroidism, mineralization defects, bone loss and fractures<sup>33</sup>. In combination with a sufficient calcium supply, vitamin D and its metabolites are able to enhance the calcium balance and facilitate mineral deposition in bone matrix<sup>34</sup>. Our recent study also demonstrated that administration of 1,25(OH)<sub>2</sub>D<sub>3</sub> to CKD mice improves the fixation of titanium implants<sup>35</sup>.

FGF23 Ab administration corrected the hyperparathyroidism of CKD mice in this study. PTH, another key factor of mineral ion homeostasis, is secreted by the chief cells of the parathyroid glands as a polypeptide and regulates the serum calcium and phosphate levels. Continuous stimulation with PTH accelerates calcium release from bone<sup>36</sup>, and leads to high bone turnover, which subsequently causes abnormal high BV/TV and high osteoid volume<sup>37</sup>. A previous study revealed that continuous infusion of bovine PTH (1–84) resulted in an increase in both osteoblast and osteoclast function, causing increased bone formation and resorption, and a net decrease in trabecular bone volume<sup>38</sup>. Selby *et al.* studied the forearms of CKD patients and found that there was a negative relationship between bone density and PTH concentration and the bone loss in these patients is related to the secondary hyperparathyroidism<sup>39</sup>. Moreover, this excess PTH directly stimulates FGF23 transcription and secretion<sup>40</sup>. In this study, we showed that FGF23 Ab administration corrected the hyperparathyroidism of CKD mice. The resulting down-regulation of PTH may contribute to the improvement of bone structures and push-in resistance of implants.

In this study, FGF23 levels were normalized upon FGF23 Ab administration. FGF23 plays a major role in balancing mineral ion homeostasis<sup>10,11</sup> and its altered activity can lead to severe disturbances in phosphate metabolism, resulting in either hyperphosphatemia or rickets<sup>10,13,14</sup>. Genetic deletion of FGF23 in mice causes severe skeletal defects<sup>10,41</sup>. In addition, FGF23 itself plays a direct role in inhibiting mineralization. Both adenoviral overexpression of FGF23 in rat calvaria cells or treatment with exogenous FGF23 peptide inhibit differentiation and mineralization of osteoblasts<sup>15,16</sup>. It is notable that phosphate levels in experimental mice were increased after treatment with FGF23 Ab. This effect is probably due, at least in part, to the inhibition of the phosphaturic activity of FGF23 on the residual kidney<sup>24</sup>. Hyperphosphatemia is a major risk for ectopic calcification<sup>24,42,43</sup>. Shalhoub *et al.* indicated that FGF23 Ab aggravates serum phosphate and artery calcification in CKD rats.

Mortality is closely related to arterial stiffness, left ventricular hypertrophy (LVH), and cardiovascular events which seriously increase the possibility to death<sup>44–46</sup>. The effects of neutralizing FGF23 Ab on the phosphaturic function of FGF23 during CKD needs to be further investigated.

We observed no significant increase in phosphate levels in CKD mice compared to the sham group. CKD mice in this study were fed with normal diet instead of the high-phosphate diet used by other researchers<sup>24</sup>. A recent report showed that injection of KRN23, a type of FGF23 Ab, into X-linked hypophosphatemia patients increases serum phosphate and 1,25(OH)<sub>2</sub>D with no other side effects<sup>47</sup>. Also, Huang *et al.* confirmed that feeding mice with a high fat diet, such as with excess in saturated fatty acids (SFA), will further augment serum phosphate level and thereby exacerbate CKD development and increase the rate of mortality<sup>48</sup>.

In summary, we successfully demonstrated that FGF23 neutralization improves bone quality and osseointegration of titanium implants in chronic kidney disease mice, indicating FGF23 is a key factor of CKD related bone diseases. FGF23 Ab administration might therefore be a potential therapeutic method to improve the skeletal health of CKD patients. Additional studies are required to suggest ways to control the increased phosphate levels.

- Al Rukhaimi, M. *et al.* Adaptation and Implementation of the "Kidney Disease: Improving Global Outcomes (KDIGO)" Guidelines for Evaluation and Management of Mineral and Bone Disorders in Chronic Kidney Disease for Practice in the Middle East Countries. *Saudi Journal of Kidney Diseases and Transplantation* **25**, 133 (2014).
- Zhang, L. *et al.* Prevalence of chronic kidney disease in China: a cross-sectional survey. *The Lancet* **379**, 815–822 (2012).
- Anand, S. *et al.* High prevalence of chronic kidney disease in a community survey of urban Bangladeshis: a cross-sectional study. *Globalization and health* **10**, 9 (2014).
- Coresh, J. *et al.* Prevalence of chronic kidney disease in the United States. *Jama* **298**, 2038–2047 (2007).
- Hallan, S. I. *et al.* International comparison of the relationship of chronic kidney disease prevalence and ESRD risk. *J Am Soc Nephrol* **17**, 2275–2284, doi:10.1681/ASN.2005121273 (2006).
- Kidney Disease: Improving Global Outcomes, C. K. D. M. B. D. W. G. KDIGO clinical practice guideline for the diagnosis, evaluation, prevention, and treatment of Chronic Kidney Disease-Mineral and Bone Disorder (CKD-MBD). *Kidney international. Supplement*, S1–130, doi:10.1038/ki.2009.188 (2009).
- Nickolas, T. L. *et al.* Bone mass and microarchitecture in CKD patients with fracture. *Journal of the American Society of Nephrology* **21**, 1371–1380 (2010).
- Lobao, R. *et al.* High prevalence of low bone mineral density in pre-dialysis chronic kidney disease patients: bone histomorphometric analysis. *Clinical nephrology* **62**, 432–439 (2004).
- Zou, H. *et al.* Effect of chronic kidney disease on the healing of titanium implants. *Bone* **56**, 410–415, doi:10.1016/j.bone.2013.07.014 (2013).
- Yoshiko, Y. *et al.* Mineralized tissue cells are a principal source of FGF23. *Bone* **40**, 1565–1573 (2007).
- Mirams, M., Robinson, B. G., Mason, R. S. & Nelson, A. E. Bone as a source of FGF23: regulation by phosphate? *Bone* **35**, 1192–1199 (2004).
- Huang, X., Jiang, Y. & Xia, W. FGF23 and Phosphate Wasting Disorders. *Bone Research* **56**, 120–132 (2013).
- White, K. E. *et al.* Autosomal dominant hypophosphatemic rickets is associated with mutations in FGF23. *Nature genetics* **26**, 345–348 (2000).
- Goji, K., Ozaki, K., Sadewa, A. H., Nishio, H. & Matsuo, M. Somatic and germline mosaicism for a mutation of the PHEX gene can lead to genetic transmission of X-linked hypophosphatemic rickets that mimics an autosomal dominant trait. *Journal of Clinical Endocrinology & Metabolism* **91**, 365–370 (2006).
- Wang, H. *et al.* Overexpression of fibroblast growth factor 23 suppresses osteoblast differentiation and matrix mineralization in vitro. *J Bone Miner Res* **23**, 939–948, doi:10.1359/jbmr.080220 (2008).
- Shalhoub, V. *et al.* Fibroblast growth factor 23 (FGF23) and alpha-klotho stimulate osteoblastic MC3T3. E1 cell proliferation and inhibit mineralization. *Calcified tissue international* **89**, 140–150 (2011).
- Larsson, T., Nisbeth, U., Ljunggren, Ö., Jüppner, H. & Jonsson, K. B. Circulating concentration of FGF-23 increases as renal function declines in patients with chronic kidney disease, but does not change in response to variation in phosphate intake in healthy volunteers. *Kidney international* **64**, 2272–2279 (2003).
- Hasegawa, H. *et al.* Direct evidence for a causative role of FGF23 in the abnormal renal phosphate handling and vitamin D metabolism in rats with early-stage chronic kidney disease. *Kidney international* **78**, 975–980 (2010).



19. Mirza, M. A., Larsson, A., Lind, L. & Larsson, T. E. Circulating fibroblast growth factor-23 is associated with vascular dysfunction in the community. *Atherosclerosis* **205**, 385–390, doi:10.1016/j.atherosclerosis.2009.01.001 (2009).
20. Abraham, B. P., Prasad, P. & Malaty, H. M. Vitamin D deficiency and corticosteroid use are risk factors for low bone mineral density in inflammatory bowel disease patients. *Digestive diseases and sciences* **59**, 1878–1884, doi:10.1007/s10620-014-3102-x (2014).
21. Gutierrez, O. *et al.* Fibroblast growth factor-23 mitigates hyperphosphatemia but accentuates calcitriol deficiency in chronic kidney disease. *Journal of the American Society of Nephrology : JASN* **16**, 2205–2215, doi:10.1681/ASN.2005010052 (2005).
22. Portillo, M. R., López, I., Juan, M., Tejero, E. A. & Almaden, Y. FGF23 and mineral metabolism, implications in CKD-MBD. *Nefrología: publicación oficial de la Sociedad Española de Nefrología* **32**, 275–278 (2012).
23. Seiler, S., Heine, G. H. & Fliser, D. Clinical relevance of FGF-23 in chronic kidney disease. *Kidney International* **76**, S34–S42 (2009).
24. Shalhoub, V. *et al.* FGF23 neutralization improves chronic kidney disease-associated hyperparathyroidism yet increases mortality. *The Journal of clinical investigation* **122**, 2543 (2012).
25. Yuan, Q. *et al.* Increased osteopontin contributes to inhibition of bone mineralization in FGF23-deficient mice. *Journal of bone and mineral research: the official journal of the American Society for Bone and Mineral Research* **29**, 693–704, doi:10.1002/jbmr.2079 (2014).
26. Erben, R. G. *et al.* Overexpression of Human PHEX Under the Human  $\beta$ -Actin Promoter Does Not Fully Rescue the Hyp Mouse Phenotype. *Journal of Bone and Mineral Research* **20**, 1149–1160 (2005).
27. Dempster, D. W. *et al.* Standardized nomenclature, symbols, and units for bone histomorphometry: a 2012 update of the report of the ASBMR Histomorphometry Nomenclature Committee. *Journal of Bone and Mineral Research* **28**, 2–17 (2013).
28. Holick, M. F. Vitamin D deficiency. *The New England journal of medicine* **357**, 266–281, doi:10.1056/NEJMr070553 (2007).
29. Pilz, S., Iodice, S., Zittermann, A., Grant, W. B. & Gandini, S. Vitamin D status and mortality risk in CKD: a meta-analysis of prospective studies. *American Journal of Kidney Diseases* **58**, 374–382 (2011).
30. Jacob, A. I., Sallman, A., Santiz, Z. & Hollis, B. W. Defective photoproduction of cholecalciferol in normal and uremic humans. *The Journal of nutrition* **114**, 1313–1319 (1984).
31. Doorenbos, C. R., van den Born, J., Navis, G. & de Borst, M. H. Possible renoprotection by vitamin D in chronic renal disease: beyond mineral metabolism. *Nature reviews. Nephrology* **5**, 691–700, doi:10.1038/nrneph.2009.185 (2009).
32. Holick, M. F. Vitamin D and bone health. *The Journal of nutrition* **126**, 1159S–1164S (1996).
33. Lips, P. Vitamin D deficiency and secondary hyperparathyroidism in the elderly: consequences for bone loss and fractures and therapeutic implications. *Endocrine reviews* **22**, 477–501 (2001).
34. Eisman, J. A. & Bouillon, R. Vitamin D: direct effects of vitamin D metabolites on bone: lessons from genetically modified mice. *BoneKey reports* **3**, 499, doi:10.1038/bonekey.2013.233 (2014).
35. Liu, W. *et al.* Vitamin d supplementation enhances the fixation of titanium implants in chronic kidney disease mice. *PLoS one* **9**, e95689, doi:10.1371/journal.pone.0095689 (2014).
36. Raisz, L. G. Bone resorption in tissue culture. Factors influencing the response to parathyroid hormone. *Journal of Clinical Investigation* **44**, 103 (1965).
37. Tamagaki, K. *et al.* Severe hyperparathyroidism with bone abnormalities and metastatic calcification in rats with adenine-induced uraemia. *Nephrology Dialysis Transplantation* **21**, 651–659 (2006).
38. Tam, C. S., Heersche, J. N., Murray, T. M. & Parsons, J. A. Parathyroid Hormone Stimulates the Bone Apposition Rate Independently of Its Resorptive Action: Differential Effects of Intermittent and Continuous Administration\*. *Endocrinology* **110**, 506–512 (1982).
39. Selby, P. L., Davies, M., Adams, J. E. & Mawer, E. B. Bone loss in celiac disease is related to secondary hyperparathyroidism. *Journal of Bone and Mineral Research* **14**, 652–657 (1999).
40. Silver, J. & Naveh-Many, T. FGF-23 and secondary hyperparathyroidism in chronic kidney disease. *Nature reviews. Nephrology* **9**, 641–649, doi:10.1038/nrneph.2013.147 (2013).
41. Bergwitz, C. & Jüppner, H. Regulation of phosphate homeostasis by PTH, vitamin D, and FGF23. *Annual review of medicine* **61**, 91–104 (2010).
42. Moe, O. W. Fibroblast growth factor 23: friend or foe in uremia? *The Journal of clinical investigation* **122**, 2354 (2012).
43. Rangiani, A. *et al.* Dentin matrix protein 1 and phosphate homeostasis are critical for postnatal pulp, dentin and enamel formation. *International journal of oral science* **4**, 189–195, doi:10.1038/ijos.2012.69 (2012).
44. London, G. M. *et al.* Arterial media calcification in end-stage renal disease: impact on all-cause and cardiovascular mortality. *Nephrology Dialysis Transplantation* **18**, 1731–1740 (2003).
45. Nitta, K. *et al.* Left ventricular hypertrophy is associated with arterial stiffness and vascular calcification in hemodialysis patients. *Hypertension research: official journal of the Japanese Society of Hypertension* **27**, 47–52 (2004).
46. Raggi, P. *et al.* Cardiac calcification in adult hemodialysis patients: A link between end-stage renal disease and cardiovascular disease? *Journal of the American College of Cardiology* **39**, 695–701 (2002).
47. Carpenter, T. O. *et al.* Randomized trial of the anti-FGF23 antibody KRN23 in X-linked hypophosphatemia. *The Journal of clinical investigation* **124**, 1587 (2014).
48. Huang, X., Lindholm, B., Stenvinkel, P. & Carrero, J. J. Dietary fat modification in patients with chronic kidney disease: n-3 fatty acids and beyond. *Journal of nephrology* **26**, 960 (2013).

## Acknowledgments

We thank Amgen Inc. for providing the FGF23 neutralizing antibody. This work was supported by grants from the National Natural Science Foundation of China (NSFC 81371173, 81321002), Sichuan Province Youth Fund (2013JQ0017), and 111 project of Ministry of Education of China, and the National Institute of Diabetes and Digestive and Kidney Diseases (NIDDK, R01- 097105) to BL.

## Author contributions

Q.Y. and B.L. designed the project. Q.Y., B.L., V.S., R.G.E. and L.Y. designed experiments. Q.Y., N.S., Y.G., W.L. and M.D. performed a significant amount of the experimental work. Q.Y., N.S., L.Y. and R.G.E. performed most of the data collection and data analysis. Q.Y. directed the study and wrote the main manuscript text and prepared figures and tables. All authors reviewed the manuscript.

## Additional information

**Competing financial interests:** The authors declare no competing financial interests.

**How to cite this article:** Sun, N. *et al.* FGF23 neutralization improves bone quality and osseointegration of titanium implants in chronic kidney disease mice. *Sci. Rep.* **5**, 8304; DOI:10.1038/srep08304 (2015).



This work is licensed under a Creative Commons Attribution-NonCommercial-NoDerivs 4.0 International License. The images or other third party material in this article are included in the article's Creative Commons license, unless indicated otherwise in the credit line; if the material is not included under the Creative Commons license, users will need to obtain permission from the license holder in order to reproduce the material. To view a copy of this license, visit <http://creativecommons.org/licenses/by-nc-nd/4.0/>